

Stable Fulde-Ferrell-Larkin-Ovchinnikov pairing states in 2D and 3D optical lattices

Zi Cai,¹ Yupeng Wang,² and Congjun Wu¹

¹*Department of Physics, University of California, San Diego, CA92093*

²*Beijing National Laboratory for Condensed Matter Physics, Institute of Physics, Chinese Academy of Sciences, Beijing 100080, P. R. China*

We present the study of the Fulde-Ferrell-Larkin-Ovchinnikov (FFLO) pairing states in the p -orbital bands in both two and three-dimensional optical lattices. Due to the quasi one-dimensional band structure which arises from the unidirectional hopping of the orthogonal p -orbitals, the pairing phase space is not affected by spin imbalance. Furthermore, interactions build up high dimensional phase coherence which stabilizes the FFLO states in 2D and 3D optical lattices in a large parameter regime in the phase diagram. These FFLO phases are stable with imposing the inhomogeneous trapping potential. Their entropies are comparable to the normal states at finite temperatures.

PACS numbers: 03.75.Ss, 05.30.Fk, 71.10.Pm, 74.20.Fg

The FFLO phases are a class of exotic Cooper pairing states exhibiting non-zero center of mass momenta [1–4], which occur in spin imbalanced systems with mismatched Fermi surfaces. However, such states are difficult to realize in solid state systems. The strong orbital effects of external magnetic fields often suppress Cooper pairing before sizable spin polarizations are reached. Moreover, because only small fractions of the mismatched Fermi surfaces can participate pairing, the FFLO states are usually fragile in 2D and 3D systems. In spite of indirect evidence in various heavy fermion compounds and organic superconductors (e.g. CeCoIn₅ [5] and λ -(BETS)₂FeCl₄ [6]), the FFLO states remain elusive.

In the cold atom community, the search for the FFLO pairing states has been attracting considerable interest [7–27]. Spin imbalanced two-component fermion systems have been prepared free of the orbital effects of magnetic fields. However, the problem of the limited pairing phase space remains, thus phase separations are observed experimentally instead of the FFLO pairing in 3D traps [26, 28]. This difficulty is avoided in 1D systems whose Fermi surfaces are points, thus spin imbalance does not affect the pairing phase space. Considerable progress has been made in quasi-1D systems of coupled optical tubes in Hulet's group [7], in which the partially polarized central regions in the tubes are observed in agreement with the prediction of the Bethe ansatz solution. However, due to the intrinsic strong quantum fluctuations in 1D, the pairing density waves, which are the smoking gun evidence for the FFLO states, cannot be long-range-ordered and thus difficult to observe.

On the other hand, orbital physics with cold atoms in optical lattices has received considerable attention, which gives rise to a variety of new states of matter with both cold bosons and fermions [29–34]. In particular, it has been recently shown that the $p_{x,y}$ -orbital band in the honeycomb lattice exhibits different properties from its p_z -orbital counterpart of graphene. These include the strong correlation effects in the flat bands (e.g. Wigner crystallization [35] and ferromagnetism [36]), quantum

anomalous Hall states [37], and the heavily frustrated orbital exchange physics [38, 39].

In this article, we combine the realization of the FFLO states and the study of orbital physics with cold atoms together. The FFLO states can be stabilized in the p -orbital bands in both 2D square and 3D cubic optical lattices. Different from the metastable p -orbital boson systems [29, 34], the p -orbital systems filled with fermions with the fully filled s -band are stable due to Pauli's exclusion principle. This work is a natural high dimensional generalization of the current experiments in Hulet's group [7]. The p_x (p_y, p_z)-orbital bands behave like orthogonally-crossed quasi-1D arrays due to their highly unidirectional hoppings. The onsite negative Hubbard interactions further build up high dimensional phase coherence over the entire lattice. It combines the advantages of the large pairing phase space of quasi-1D systems and the high dimensional phase coherence.

The anisotropic p -orbital bands possess the quasi-1D like structures with perfect nesting at general fillings and spin imbalance. For simplicity, we start with the 2D case. The similar physics applies to the 3D cubic lattice as well. We present the p -band Hamiltonian as

$$H_0 = t_{\parallel} \sum_{\vec{r}, \alpha} \left\{ p_{x, \alpha}^{\dagger}(\vec{r}) p_{x, \alpha}(\vec{r} + \hat{e}_x) + p_{y, \alpha}^{\dagger}(\vec{r}) p_{y, \alpha}(\vec{r} + \hat{e}_y) \right\} - \mu \sum_{\vec{r}, \alpha} n_{\alpha}(\vec{r}) - \frac{h}{2} \sum_{\vec{r}} \{ n_{\uparrow}(\vec{r}) - n_{\downarrow}(\vec{r}) \}, \quad (1)$$

where α refers to spin index; h controls spin imbalance; $n_{\alpha}(\vec{r}) = p_{x, \alpha}^{\dagger}(\vec{r}) p_{x, \alpha}(\vec{r}) + p_{y, \alpha}^{\dagger}(\vec{r}) p_{y, \alpha}(\vec{r})$ is the particle number of spin α . Only the longitudinal σ -bonding (t_{\parallel}) term is kept which describes the hopping between p -orbitals along the bond direction as depicted in Fig. 1 (a). t_{\parallel} is positive because of the odd parity of the p -orbitals. The transverse π -bonding term with the hopping integral t_{\perp} is neglected, which describes the hopping between p -orbitals perpendicular to the bond direction as depicted in Fig. 1 (b).

In spite of the 2D lattice structure, the p -orbital band

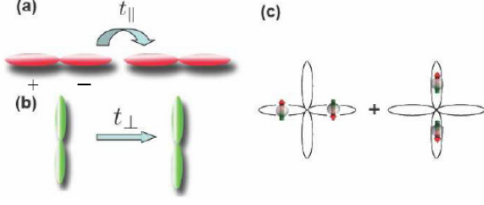


FIG. 1: (Color online) (a) and (b) describe the longitudinal hopping t_{\parallel} -term and the transverse t_{\perp} -term of the p -orbitals, respectively. (c) The pairing hopping term in Eq. (2) locks the phases of two onsite intra-orbital pairings in the p_x and p_y -orbitals.

structure of Eq. 1 remains quasi-1D-like as depicted in Fig. 2 (a). The $p_x(p_y)$ -orbital band disperses along the $x(y)$ -direction, respectively, but does not along the $y(x)$ -direction. The Fermi surfaces are vertical (p_x) and horizontal (p_y) lines across the entire Brillouin zone. For the arbitrary filling and spin imbalance, the Fermi surfaces of spin up and down fermions have the perfect nesting. Consequentially, spin imbalance *does not* suppress the pairing phase volume. The high dimensional p -orbital systems have the same advantage as that in 1D systems.

The important feature of the 2D p -orbital systems for the FFLO states is that the onsite negative Hubbard interactions build up the 2D phase coherence. The interactions are represented in the standard two-orbital Hubbard model as

$$H_{int} = \sum_{\vec{r}} U \left[n_{x\uparrow}(\vec{r}) n_{x\downarrow}(\vec{r}) + n_{y\uparrow}(\vec{r}) n_{y\downarrow}(\vec{r}) \right] - \sum_{\vec{r}} J \left[\vec{S}_x(\vec{r}) \cdot \vec{S}_y(\vec{r}) - \frac{1}{4} n_x(\vec{r}) n_y(\vec{r}) \right] + \sum_{\vec{r}} \Delta \left[p_{x\uparrow}^\dagger(\vec{r}) p_{x\downarrow}^\dagger(\vec{r}) p_{y\downarrow}(\vec{r}) p_{y\uparrow}(\vec{r}) + h.c. \right], \quad (2)$$

where $U = g \int dr |\psi_{p_{x,y}}(\vec{r})|^4 < 0$ and g is the contact interaction in the s -wave scattering approximation. J and Δ satisfy $J = \frac{2U}{3} < 0$ and $\Delta = \frac{U}{3} < 0$ [36]. The negative U -term gives rise the dominant intra-orbital singlet pairings in the p_x and p_y -orbitals, defined as

$$\Delta_x(\vec{r}) = \langle G | p_{x\uparrow}(\vec{r}) p_{x\downarrow}(\vec{r}) | G \rangle, \quad \Delta_y(\vec{r}) = \langle G | p_{y\uparrow}(\vec{r}) p_{y\downarrow}(\vec{r}) | G \rangle, \quad (3)$$

where $|G\rangle$ is the mean field pairing ground states. The J -term induces the inter-orbital singlet pairing between p_x and p_y -orbitals. However, because the Fermi surfaces of p_x and p_y -orbitals are orthogonal, the inter-orbital pairing is unfavorable.

The pair hopping Δ -term in Eq. 2 can be considered as the internal Josephson coupling to lock the phases of two intra-orbital pairings Δ_x and Δ_y . As a result, the motion of Cooper pairs are 2D-like in spite of the quasi 1D-like single fermion hopping. To clarify the pairing symmetry,

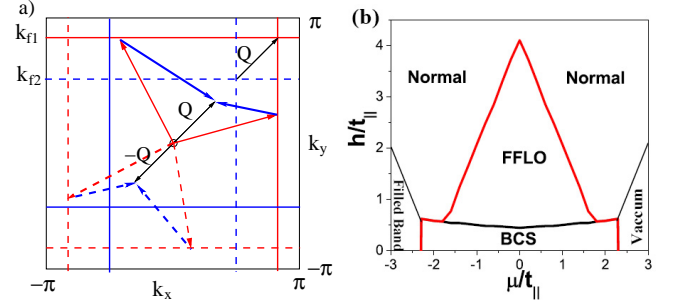


FIG. 2: (Color online) (a) The nesting of the p -orbital Fermi surfaces ensures that all of the Fermi surfaces are paired at a general filling and spin imbalance. The Fermi surfaces of the $p_x(p_y)$ -orbitals are vertical (horizontal) lines; those of the majority (minority) spins are marked red (blue). Fermi surfaces marked with solid (dashed) lines are paired with the center of mass momentum $\pm\vec{Q}$, respectively. The red and blue arrows represents the Fermi wavevectors of spin up and down fermions participating Cooper pairing. (b) The 2D phase diagram from the B-de G solution as chemical potential μ and the magnetic field h with $U/t_{\parallel} = -1.5$.

we first consider two fermions on the same site to gain some intuition. The s -wave Feshbach resonances forbid spin triplet channel and induce a spin singlet pairing. In the spin singlet channel, their orbital wavefunctions are symmetric as $p_x^2 + p_y^2$, $p_x^2 - p_y^2$ and $p_x p_y$ respectively. The first one has energy $U + \Delta = 4U/3$, while the later two are degenerate with energy $U - \Delta = J = 2U/3$. From this simple analysis, we can see that the system favors pairing with $p_x^2 + p_y^2$ orbital symmetry (as shown in Fig. 1(c)), while pairing with other two symmetries are suppressed, which can be verified by the numerical results below.

We have performed calculations based on the self-consistent Bogoliubov-de Gennes (B-deG) solution to study the competition among the FFLO state, the BCS state and the normal state as presented in Fig. 2 (b). To synchronize the phases of $\Delta_x(\vec{r})$ and $\Delta_y(\vec{r})$ on each site, their center of mass wavevectors in the FFLO states have to be the same. This can be achieved by choosing the pair density wavevectors along the diagonal direction $\pm\vec{Q}$ defined as $\vec{Q} = (\delta k_f, \delta k_f)$ where $\delta k_f = k_{f1} - k_{f2}$, and $k_{f1,2}$ are Fermi wavevectors of the majority and minority spins as indicated in Fig. 2 (a). By the symmetry of the square lattice, $\vec{Q}' = \pm(\delta k_f, -\delta k_f)$ are another possible choice of pair density wavevector. We consider the simplest Larkin-Ovchinnikov (LO) states with one pair of Cooper pair momenta $\pm\vec{Q}$, with the sinusoidal order parameter configuration as

$$\Delta_x(\vec{r}) = \Delta_y(\vec{r}) = |\Delta| \cos(\vec{Q} \cdot \vec{r}). \quad (4)$$

The LO state breaks both translational and the 4-fold lattice rotational symmetries. We have performed unbiased real space B-de G calculations without specifying the FFLO momentum in the initial conditions but rather

starting from a configuration with uniform pairing. The FFLO momentum Q in the above analysis is obtained when the numerical convergence is arrived. Compared with the phase diagram of spin-imbalanced fermions in the s -orbital band, the FFLO phase in our p -orbital band system exists in a much larger regime in the phase diagram sandwiched between the fully paired BCS phase and the fully polarized normal phase.

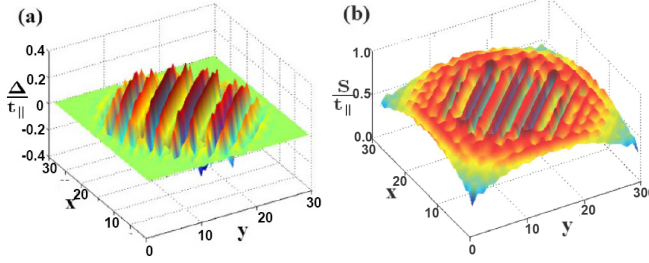


FIG. 3: (Color online) The B-de G solution of the p -orbital FFLO state in a 30×30 lattice with a weak confining trap. (a) The order parameter distribution of $\Delta_x(\vec{r})$ oscillates along the $[11]$ -direction. (b) The spin density distribution $S_z(\vec{r})$ peaks around the gap nodes.

Next we study a more realistic situation, the effects of the soft confining potential to the p -orbital FFLO states, by performing self-consistent real space B-de G calculations. We consider a 30×30 lattice with the harmonic trapping potential $V_{ex} = A(r/a)^2$ where $A/t_{\parallel} = 5 \times 10^{-3}$; r is the distance from the trap center; a is the lattice constant. The real space distribution of order parameter $\Delta_x(\vec{r})$ is shown in Fig.3 (a) with the parameters chosen as $h/t_{\parallel} = 3$, $U/t_{\parallel} = -3$ and $\mu = 0$. Clearly Δ_x oscillates along the $[11]$ -direction in agreement with the previous analysis. To verify Eq. 4, we further calculate the difference between the pairing orders in different orbitals. In the bulk, the relation that $\Delta_x(\vec{r}) = \Delta_y(\vec{r})$ is well-satisfied. The difference between $\Delta_x(\vec{r})$ and $\Delta_y(\vec{r})$ is only important at the boundary which breaks the symmetry between the p_x and p_y -orbitals. The spin density distribution $s_z(\vec{r}) = n_{\uparrow}(\vec{r}) - n_{\downarrow}(\vec{r})$ is depicted in Fig. 3 (b). It peaks around the gap nodes, which is consistent with the fact that spin polarization suppresses Cooper pairing.

Next we discuss the effect of the small π -bonding t_{\perp} , which has been neglected above but always exists in realistic systems. The t_{\perp} -term restores the 2D nature of the Fermi surfaces and suppresses the perfect nesting, therefore it is harmful to the FFLO states. Our numerical result indicates that the FFLO state remains stable at small values of t_{\perp} . For example, with $U/t_{\parallel} = -3$, $h/t_{\parallel} = 3$ and $\mu = 0$, the FFLO state survives until t_{\perp}/t_{\parallel} reaches 0.12. Beyond this value, it changes to the normal state through a first order phase transition. As calculated in Ref. [30], with the optical potential depth $V_0/E_R \approx 15$, t_{\parallel} is at the order of $0.1E_R$ and $t_{\perp}/t_{\parallel} \approx 5\%$.

Increasing optical potential depth further suppresses t_{\perp} , thus there is a large parameter regime to stabilize the FFLO states.

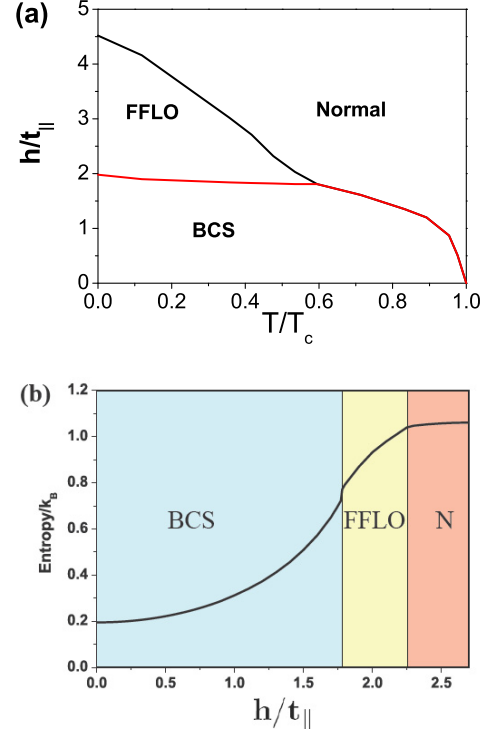


FIG. 4: (Color online) (a) The finite temperature phase diagram for the 3D p -orbital bands with $U/t_{\parallel} = -2.4$, and $\mu = 0$. $T_c/t_{\parallel} = 0.84$ is the critical temperature for the BCS state. (b) The entropy density S/k_B v.s. h/t_{\parallel} at a finite temperature of $T/t_{\parallel} = 0.4$ with parameters $\mu = 0$ and $U/t_{\parallel} = -2.4$.

The physics of the FFLO states in the p -orbital bands in the 3D cubic optical lattices is similar. The 3D p -orbital Hamiltonian is similar to Eq. 1 and Eq. 2, and further augmented by a new orbital p_z . The pair density wavevectors are along the body diagonal directions, *i.e.*, the $\pm[111]$ or other equivalent directions. Similar to the Eq.(4), the FFLO state in 3D cubic optical lattice is characterized by the sinusoidal order parameter configuration as:

$$\Delta_x(\vec{r}) = \Delta_y(\vec{r}) = \Delta_z(\vec{r}) = |\Delta| \cos(\vec{Q} \cdot \vec{r}). \quad (5)$$

where $\vec{Q} = (\pm\delta k_f, \pm\delta k_f, \pm\delta k_f)$ are along the body-diagonal directions.

In the 3D p -orbital bands, the long range ordered BCS and FFLO states survive at finite temperatures, and mean-field theory works qualitatively well. We present the finite temperature phase diagram of the competing orders at $U/t_{\parallel} = -2.4$ and $\mu = 0$ in Fig. 4 (a). The FFLO state can also survive to finite critical temperatures at the same order of T_c . We further present the

entropy S v.s. h for different competing orders at a fixed temperature $T/t_{\parallel} = 0.4$ in Fig. 4 (b). The FFLO state has a large value of entropy density due to the extra unpaired majority fermions, which interpolate between the BCS and the fully polarized normal state. This greatly increases the accessibility of the FFLO state in the cold atom optical lattices. The transition between the BCS and the FFLO states is first order as indicated by the discontinuity of entropy in Fig. 4 (b).

At last, we discuss experiment realizations and detections. The p -band fermion systems can be realized by first preparing enough number of atoms to fully fill the s -orbital band, thus the extra particles will fill the p -bands. The attractive interaction can be achieved through Feshbach resonances in lattices [7, 40], whose strength can be tuned comparable to the band width of $4t_{\parallel} \approx 0.5E_R$ at $V_0/E_R \approx 15$ [30], but still small compared to band gaps which is around several E_R . Our work predicts a large stable parameter regime for the FFLO states. These states can be detected by many methods [21, 23, 24], such as the direct imaging of the density profile oscillations of each of the fermion components, the rf spectroscopy measurement on the collective modes, converting Cooper pairs into molecules and measuring their momenta, the shot-noise correlation of the Fermi momenta between \vec{k} and $-\vec{k} \pm \vec{Q}$, etc. In particular, the recent development of the *in situ* imaging methods with the single site resolution [41, 42] can be used to accurately determine the spatial oscillation of the FFLO states.

In summary, we have studied the competing orders among the FFLO, the BCS, and the normal states in the spin imbalanced p -orbital band systems in both 2D and 3D. The FFLO states are stabilized by the combined effects of the quasi-1D Fermi surfaces and the high dimensional phase coherence built up by the inter-orbital interactions. The pairing density wavevectors are along the diagonal directions to facilitate the maximal inter-orbital pairing phase coherence. The FFLO states are robust with many realistic experimental effects including the confining trap, the small transverse π -bonding, and finite temperatures. It would be nice to realize the 2D and 3D stable FFLO phases in the p -orbital bands in optical lattices which have not been identified in solid state systems yet.

Z.C. and C. W. are supported by the Sloan Research Foundation, NSF-DMR-03-42832 and AFOSR-YIP. Y. P. W. is supported by NSFC and 973-project of MOST (China).

[1] P. Fulde and R. A. Ferrell, Phys. Rev. **135**, A550 (1964).
[2] A. I. Larkin and Y. N. Ovchinnikov, Sov. Phys. – JETP **20**, 762 (1965).
[3] R. Casalbuoni and G. Nardulli, Rev. Mod. Phys. **76**, 263 (2004).

[4] Y. Matsuda and H. Shimahara, J. Phys. Soc. Jpn. **76**, 051005 (2007).
[5] H. A. Radovan *et al.*, Nature **425** 51 (2003). A. Bianchi *et al.*, Phys. Rev. Lett. **91** 187004 (2003). K. Kakuyanagi *et al.*, Phys. Rev. Lett. **94** 047602 (2005).
[6] S. Uji, H. Shinagawa, T. Terashima, T. Yakabe, Y. Terai, M. Tokumoto, A. Kobayashi, H. Tanaka and H. Kobayashi, Nature **410**, 908 (2001).
[7] Y. Liao, A. S. C. Rittner, T. Paprotta, W. H. Li, G. B. Partridge, R. G. Hulet, S. K. Baur and E. J. Mueller, Nature **467**, 567 (2010).
[8] W. Ketterle and M. W. Zwierlein, arXiv.org:0801.2500.
[9] Y. L. Loh and N. Trivedi, Phys. Rev. Lett. **104**, 165302 (2010).
[10] E. Zhao and W. V. Liu, Phys. Rev. A **78**, 063605 (2008).
[11] T. K. Koponen, T. Paananen, J. P. Martikainen, and P. Törmä, Phys. Rev. Lett. **99**, 120403 (2007).
[12] T. K. Koponen, T. Paananen, J. P. Martikainen, M. R. Bakhtiari and P. Törmä, N. J. Phys. **10**, 045014 (2008).
[13] M. M. Parish, S. K. Baur, E. J. Mueller, and D. A. Huse, Phys. Rev. Lett. **99**, 250403 (2007).
[14] A. E. Feiguin and F. Heidrich-Meisner, Phys. Rev. B **76**, 220508 (2007).
[15] G. G. Batrouni, M. H. Huntley, V. G. Rousseau, and R. T. Scalettar, Phys. Rev. Lett. **100**, 116405 (2008).
[16] J. M. Edge and N. R. Cooper, Phys. Rev. Lett. **103**, 065301 (2009).
[17] X.-J. Liu, H. Hu, and P. D. Drummond, Phys. Rev. A **76**, 043605 (2007).
[18] T. Paananen, T. K. Koponen, P. Törmä, and J. P. Martikainen, Phys. Rev. A **77**, 053602 (2008).
[19] A. Lüscher, R. M. Noack, and A. M. Läuchli, Phys. Rev. A **78**, 013637 (2008).
[20] P. Kakashvili and C. J. Bolech, Phys. Rev. A **79**, 041603 (2009).
[21] K. Yang, Phys. Rev. Lett. **95**, 218903 (2005).
[22] J. Kinnunen, L. M. Jensen, and P. Törmä, Phys. Rev. Lett. **96**, 110403 (2006).
[23] T. Mizushima, K. Machida, and M. Ichioka, Phys. Rev. Lett. **94**, 060404 (2005).
[24] M. R. Bakhtiari, M. J. Leskinen, and P. Törmä, Phys. Rev. Lett. **101**, 120404 (2008).
[25] P. Nikolić, A. A. Burkov, and A. Paramekanti, Phys. Rev. B **81**, 012504 (2010).
[26] G. B. Partridge, W. H. Li, Y. A. Liao, and R. G. Hulet, Phys. Rev. Lett. **97**, 190407 (2006).
[27] L. Radzihovsky, D. E. Sheehy Rep. Prog. Phys. **73**, 076501 (2010).
[28] M. W. Zwierlein *et al.*, Nature (London) **442**, 54 (2006).
[29] T. Mueller, S. Foelling, A. Widera, and I. Bloch, Phys. Rev. Lett. **99**, 200405 (2007).
[30] A. Isacsson and S. M. Girvin, Phys. Rev. A **72**, 053604 (2005).
[31] W. V. Liu and C. Wu, Phys. Rev. A **74**, 13607 (2006).
[32] A. B. Kuklov, Phys. Rev. Lett. **97**, 110405 (2006).
[33] V. M. Stojanović, C. Wu, W. V. Liu and S. Das Sarma, Phys. Rev. Lett. **101**, 125301 (2008).
[34] G. Wirth, M. Ölschläger, A. Hemmerich, Nat. Phys. **7**, 147153 (2011).
[35] C. Wu, D. Bergman, L. Balents, and S. Das Sarma, Phys. Rev. Lett. **99**, 070401 (2007).
[36] S. Z. Zhang, H. H. Hung, and C. Wu, Phys. Rev. A **82**, 053618 (2010).

- [37] M. Zhang, H. H. Hung, C. W. Zhang and C. Wu, Phys. Rev. A **83**, 023615 (2011).
- [38] C. Wu, Phys. Rev. Lett. **100**, 200406 (2008).
- [39] C. W. Chern and C. Wu arXiv:1104.1614.
- [40] J. K. Chin, D. E. Miller, Y. Liu, C. Stan, W. Setiawan, C. Sanner, K. Xu and W. Ketterle, Nature (London) **443**, 961 (2006).
- [41] N. Gemelke, X. Zhang, C. Hung, and C. Chin, Nature **460**, 995 (2009).
- [42] W. S. Bakr, J. I. Gillen, A. Peng, S. Fölling, and M. Greiner, Nature (London) **462**, 74 (2009).